Neurotoxicity Research (2022) 40:763–774
https://doi.org/10.1007/s12640-022-00509-3

ORIGINAL ARTICLE

Depletion of B7-H4 from C3H10 T1/2 Mesenchymal Stem Cells Attenuates their Immunomodulatory Therapy in Experimental Autoimmune Encephalomyelitis Mice

Hao Li[1] · Simao Sun[1,5] · Zhou Yin[1,6] · Shugang Cao[1] · Xiaopei Ji[1] · Xiaoyu Duan[1] · Hanqing Gao[1] · Mingyuan Wang[4] · Qi Fang[1,2] · Wanli Dong[1] · Xueguang Zhang[2,3] · Yanzheng Gu[2,3] · Qun Xue[1,2,3]

Received: 17 February 2022 / Revised: 6 April 2022 / Accepted: 9 April 2022 / Published online: 25 April 2022

Abstract

Considering the controversial issue of whether MSC therapy is effective in the treatment of multiple sclerosis, it is important to seek more powerful data to clarify the effect of MSCs. B7-H4 is a unique costimulatory molecule that belongs to the B7 ligand family and is broadly expressed in both lymphoid and non-lymphoid tissues. Previous studies have shown that B7-H4 is involved in regulating the progression of autoimmune diseases. However, its role in MSCs and stem cell transplantation remains unclear. In this study, we focus on C3H10 T1/2 cells, which are mouse-derived mesenchymal stem cells. And we investigated the role of B7-H4 in C3H10 T1/2 cells and explored its underlying mechanisms. As a result, downregulation of B7-H4 induced apoptosis and impaired the cell proliferation of C3H10 T1/2 cells. Further results showed that cells were arrested in the G0/G1 phase after knockdown of B7-H4. Furthermore, an EAE model was induced in female C57BL/6 mice by injecting MOG 35–55, and we investigated the effect of C3H10 T1/2 cell transplantation for the EAE model after downregulation of B7-H4 in vivo. We found that C3H10 cells can migrate to the area of spinal cord lesions, and depletion of B7-H4 attenuated the immunoregulatory effect of C3H10 T1/2 cells in vivo. Together, our findings suggest that B7-H4 is important for C3H10 cells to exert neurorestoration and therefore may be a potential molecular target for stem cell transplant strategies.

Keywords B7-H4 · C3H10 T1/2 cells · Stem cell transplantation · Autoimmune diseases

Hao Li, Simao Sun, and Zhou Yin contributed equally to this work.

✉ Yanzheng Gu
gyz_1982@yeah.net

✉ Qun Xue
qxue_sz@163.com

[1] Department of Neurology, The First Affiliated Hospital of Soochow University, 188 Shizi Road, Suzhou, China

[2] Jiangsu Institute of Clinical Immunology, Jiangsu Key Laboratory of Clinical Immunology, The First Affiliated Hospital of Soochow University, Soochow University, Suzhou 215006, China

[3] Jiangsu Key Laboratory of Gastrointestinal Tumor Immunology, The First Affiliated Hospital of Soochow University, 708 Renmin Road, Suzhou, China

[4] Suzhou Red Cross Blood Center, Suzhou 215006, China

[5] Department of Neurology, Loudi Central Hospital, Loudi, Hunan Province 417000, China

[6] Department of Neurology, 521 Hospital of NORINCO Group, Xi'an, China

Abbreviations

MS	Multiple sclerosis
CNS	Central nervous system
MSCs	Mesenchymal stem cells
EAE model	Experimental autoimmune encephalomyelitis model
GFP	Green fluorescent protein
FBS	Fetal bovine serum
H&E staining	Hematoxylin and eosin staining
LFB staining	Luxol fast blue staining
NC	Negative control

Introduction

Multiple sclerosis (MS) is one of the most prevalent common neurologic disorders leading to chronic disability, and it is considered an autoimmune disorder that causes a chronic inflammatory and demyelinating condition of the brain and spinal cord of the central nervous system (CNS) (Gugliandolo et al. 2020). MS is characterized by the destruction of

oligodendrocytes and neurons, resulting in demyelination with concomitant axonal (Vaughn et al. 2019). Genetic, environmental, and immune factors are believed to act synergistically in the pathogenesis of MS. Population and epidemiological studies have indicated that nearly 85% of MS patients present with a type called relapsing–remitting multiple sclerosis relapsing–remitting course of the disease (RRMS) (Faissner et al. 2019), which seriously threatens the quality of life of MS patients and affects their functionality in numerous ways. The available medications only provide symptomatic relief but do not stop the progression of the disease (Pfeuffer et al. 2016; Levy et al. 2020). At present, the main challenge for MS therapy is to find treatments that can reduce the rate of relapsing and improve the prognosis (Pfeuffer et al. 2016). A growing amount of preclinical and clinical training has supported that mesenchymal stem cell (MSC) transplantation can improve central nervous system (CNS) restoration and improve functional neurological signs (Gugliandolo et al. 2020). MSC can reduce inflammation and modulate the immune system, while the corresponding mechanism involved in MSC immunomodulation has not yet been fully found.

B7-H4, also known as B7x, B7S1, VTCN1, is a costimulatory protein that negatively regulates the immune response of T cells and promotes immune escape by inhibiting proliferation, secretion of cytokines, and cell cycle of T cells (Jeon et al. 2014; Greaves and Gribben 2013; Song et al. 2020). Furthermore, B7-H4 is found to be involved in the pathogenesis of MS. In EAE models, disease severity is improved by blocking B7-H4 or B7-H4 knockout mice (Prasad et al. 2003). Therapeutic treatment with B7-H4-Ig effectively improved the progress of chronic EAE and relapsed EAE (Podojil et al. 2013). B7-H4 is broadly expressed in lymphoid and non-lymphoid tissues (Collins et al. 2005). Our previous study demonstrated that high expression of B7-H4 in human bone marrow stromal cells (hBMSCs) plays an important role in inhibiting T cell proliferation through induction of cell cycle arrest and inhibition of nuclear translocation of NF-kappa B (Xue et al. 2010).

The current study aimed to investigate the role of B7-H4 in C3H10T1/2 mesenchymal stem cells and its impact on inflammatory infiltration and demyelination changes after transplanted cells in an EAE model. A better understanding of the characteristics of B7-H4 in C3H10 cells may provide novel insights into stem cell therapy for MS.

Materials and Methods

Animals

Female C57BL/6 mice (17–21 g, 10–12 weeks old) were purchased from Shanghai SLAC Laboratory Animal Co., Ltd. (Shanghai, China). All animals had free access to food and water under controlled conditions (12/12 h light/dark cycle, 40–70% humidity, 23 ± 3 °C). All animals were housed and handled according to the criteria of the National Institute of Health Guide for the Care and Use of Laboratory Animals (NIH Publications No. 8023, revised 2011). All experimental protocols were approved by the Ethics Committee of the First Affiliated Hospital of Soochow University and its Institutional Animal Care Committee.

Experimental Design

To detect the role of B7-H4 in C3H10 cells after the induced EAE model, cells were divided into the following three groups: C3H10 was infected with the lentivirus vector group (C3H10), C3H10 was infected with the lentivirus-containing shRNA-NC group (C3H10-NC), C3H10 was infected with the lentivirus-containing shRNA group (C3H10-B7-H4sh). The mice were divided into the following five groups: normal group, EAE group, EAE + C3H10 transplantation group (C3H10), EAE + C3H10-NC group (C3H10-NC), EAE + C3H10-B7-H4sh group (C3H10-B7-H4sh).

Reagents

The following antibodies were purchased from Proteintech: Ms. mAb for the caspase3 antibody (Cat No. 66470–2-LG); Rb pAb for the caspase9 antibody (Cat No. 10380–2-AP); Rb pAb for the Cyclin D1 antibody (Cat No. 26939–1-AP). The following antibodies were purchased from Santa Cruz: Rb pAb for the B7-H4 antibody (sc-68872); Ms. mAb for the Bcl-2 antibody (sc-7382). The Rb mAb for the Bax antibody (ab182733) was purchased from Abcam. Secondary antibodies for Western blot analysis, including anti-rabbit IgG-HRP (7074 s) and anti-mouse IgG-HRP (7076 s), were purchased from Cell Signaling Technology. Secondary antibodies for immunofluorescence were purchased from Invitrogen and included the following: Cy3-conjugated goat anti-mouse secondary antibody (A10521) and Cy3-conjugated goat anti-rabbit secondary antibody (A10520).

Cell Culture

Cell lines C3H10 T1/2 were obtained from the Chinese Academy of Sciences Cell Research Institute (Shanghai, China) and cultured in MEM medium (Genom Co., LTD, Hangzhou, China) supplemented with 10% fetal bovine serum (FBS), 100 U/ml penicillin, and 100 µg/ml streptomycin. All cells were incubated at 37 ℃ in a humidified atmosphere containing 5% CO_2.

Construction of a Specific shRNA Against B7-H4

A specific shRNA lentivirus against B7-H4 was obtained from GenePharma (GenePharma Co., LTD, Shanghai, China) to eliminate the expression of B7-H4. Four different B7-H4 target sequences were used in this study and are listed in Supplementary Table 1 (Genebank: No. NM178594.2). The efficiency of the four shRNAs was tested to suppress B7-H4 expression, and the most efficient shRNA was used in this study. For in vitro B7-H4 downregulation experiments, the shRNA mentioned above was packaged into a lentivirus vector that can produce a green fluorescent protein (GFP). The lentiviral titer of the packaged shRNA was 3×10^8 UT/ml.

EAE Model

The demyelinating EAE model was induced by MOG-35 as previously reported (Jia et al. 2021). MOG (35–55) or myelin oligodendrocyte glycoprotein (MOG) 35–55 is a minor component of CNS myelin. MOG (35–55) produces a relapsing–remitting neurological disease with extensive plaque-like demyelination, common to manifestations of multiple sclerosis. MOG (35–55) induces strong T and B cell responses and is highly encephalitogenic. MOG (35–55) induces T-cell-mediated multiple sclerosis in animal models. Three hundred micrograms of MOG 35–55 polypeptide power (GL Biochem, Shanghai, China) was dissolved in 50 µl of PBS and emulsified in 50 µl of complete Freund adjuvant (Sigma, St. Louis, MO, USA) supplemented with 500 µg Mycobacterium tuberculosis (Difco, Detroit, MI). Emulsification was performed using a medical infusion tee and a medical syringe (5 ml), producing a white emulsion. Ten-week-old female C57BL/6 mice were injected under the armpit and the total injection amount for each mouse was 100 µl. Furthermore, mice were injected intraperitoneally (i.p.) with 200 ng of purified Bordetella pertussis toxin (Biosource, Shanghai, China) on days 0 and 1.

Assessment of the EAE Model

The clinical scores of the behavioral manifestations were evaluated using a scale ranging from 0 to 5 following the criteria shown in Supplementary Table 2, with a 0.5 point difference between the two criteria.

Stable Infection by Lentivirus in C3H10 Cells

C3H10 cells were diluted to 40.000 cells/ml in MEM medium (Genom Co., LTD, Hangzhou, China) supplemented with 10% fetal bovine serum (FBS). Cells were then seeded in 12-well plates and incubated in 5% CO_2 and 95% air at 37 ℃. Each 100 µl lentivirus (shRNA or shRNA-NC) was dissolved in 400 µl MEM medium (supplemented with 10% FBS and 2.5 µg Polybrene) for infection. After incubation for 24 h, the medium was replaced with a fresh medium containing 10% FBS and incubated for another 24 h. Using a fluorescence microscope, cells infected with lentivirus were selected with 2 µg/ml Zeocin (Invitrogen, Carlsbad, CA, USA) until infection efficiency reaches more than 90%. Stable cloned cells are used in the following experiments.

Western Blot Analysis

Transfected cells were treated with trypsin and washed three times with ice-cold PBS. Total cell protein was extracted and then quantified using an enhanced BCA protein assay kit (Beyotime, Shanghai, China). Equal amounts of prepared proteins (15 µg/lane) were loaded onto an SDS–polyacrylamide gel, separated, and then electrophoretically transferred to polyvinylidene difluoride membranes (PVDF) (Univ-Bio Co., LTD, Shanghai, China), which were blocked with 5% fat-free milk for 1 h at room temperature. The membrane was then incubated with primary antibody overnight at 4 ℃. The titers of the antibodies used in immunoblots were as follows: Rb pAb to the B7-H4 antibody (Santa Cruz, sc-68872, 1:500 dilution), Ms. mAb to Bcl-2 antibody (Santa Cruz, sc-7382, 1:500 dilution), Rb mAb to Bax antibody (Abcam, ab182733, 1:1000 dilution), Ms. mAb to caspase3 antibody (Proteintech, Cat No. 66470–2-LG, 1:1000 dilution), Rb pAb to caspase9 antibody (Proteintech, Cat No. 10380–2-AP, 1:1000 dilution), Rb pAb to Cyclin D1 antibody (Proteintech, Cat No. 26939–1-AP, 1:1000 dilution). Meanwhile, β-tubulin or β-actin were detected as a loading control. The membranes were probed with HRP-conjugated secondary antibodies (Pierce, Rockford, IL, USA) for 1 h. We revealed the band signals via an enhanced chemiluminescence (ECL) kit (New Cell & Molecular Biotech Co., LTD, Shanghai, China). Finally, the relative quantities of proteins were analyzed using ImageJ (NIH, Bethesda, MD, USA).

Immunofluorescent Analysis

Mice were anesthetized with 4% chloral hydrate (0.1 ml/10 g) and fixed with 4% paraformaldehyde by heart perfusion. The prefixed mouse spinal cord was removed and further fixed in 4% paraformaldehyde for 24 h at 4 ℃. The spinal cords were dehydrated with 10%, 20%, and 30% sucrose solution respectively for 12 h and then cut into a 10 µm section. Similarly, cells were fixed with 4% paraformaldehyde. The section and cells were then probed with primary antibodies and appropriate secondary antibodies. The titers of the antibodies used in immunofluorescence were as follows: Rb pAb to antibody B7-H4 (Santa Cruz, sc-68872, 1:100 dilution), Rb mAb to Iba1 antibody (Abcam, ab178846, 1:200 dilution), Rb mAb to CD3 antibody

(Abcam, ab135372, 1:200 dilution), Rb mAb to CD20 antibody (Abcam, ab64088, 1:200 dilution), Rb mAb to PD-L1 antibody (Abcam, ab213524, 1:200 dilution). Normal rabbit IgG was used as negative controls for the immunofluorescence assay. Cell nuclei were stained with DAPI mounting medium. Finally, the sections and cells were observed by fluorescence microscope (TCS SP5, Leica Microsystems, Germany).

Apoptosis Assay

Apoptosis assays were performed using the Annexin V-PE/7-ADD Kit (BD Biosciences, San Jose, CA, USA). Briefly, each group of cell samples was stained with Annexin V-PE and 7-ADD according to the manufacturer's instructions. Fluorescence signals from 0.5 to 1×10^6 cells were evaluated using flow cytometry and the apoptosis rate was determined by flow cytometry.

Cell Proliferation Assay

Cell viability was assessed with the Cell Counting Kit (CCK)-8 (Fcmacs Biotechnology Co., LTD, Nanjing, China). Briefly, each group of cells (1×10^4 cells/well) was seeded in each 96-well plate. They were incubated for 1–4 days. CCK-8 was added to each well and cells were incubated for 3 h at 37 ℃. The optical density (OD) at 450 nm in each well was measured using a UV spectrophotometer (Beckman, USA). All experiments were carried out in triplicate.

Cells C3H10, C3H10-NC, and C3H10-B7-H4sh in the log phase of growth (5×10^3 cells/well) were seeded in 24-well plates. After seeding, cells were counted for 0–5 days.

Cell Cycle Assay

Each group of cells was harvested 24–48 h after infection. Cell cycle assays were then performed using the cell cycle detection Kit (HaiGene Co., LTD, China) according to the manufacturer's instructions. Briefly, each group of cells ($2–10 \times 10^5$ cells) was harvested. The cells were then fixed in 1 ml of 70% ethanol at −20 ℃ overnight. Cells were resuspended and thoroughly mixed with 1 ml of DNA staining solution by vortexing for 5–10 s. After incubation for 30 min at room temperature, the cell cycle distribution was analyzed by flow cytometry.

Histopathological Analysis

Spinal cords were removed from the mice and fixed with 4% paraformaldehyde for 24 h at 4 ℃. The extent of inflammation and demyelination was assessed using hematoxylin and eosin (H&E) and luxol fast blue (LFB) staining, respectively. Inflammatory infiltration was observed in H&E staining sections, and the semiquantitative criteria for the extent of inflammation were as follows: 0, no inflammatory cell infiltration or occasional inflammatory cell infiltration; 1, inflammatory cells infiltrated only around the blood vessels and spinal cord membrane; 2, a small number of inflammatory cells infiltrated in the parenchyma; 3, moderated inflammatory cells infiltrated in the parenchyma; 4, a large number of inflammatory cells infiltrated in the parenchyma. Demyelination was observed in the LFB staining sections and the semiquantitative criteria of the extent of demyelination were as follows: 0, no myelin injury; 1, occasional myelin injury; 2, slightly scattered demyelination; 3, moderately large area myelin loss; 4, severe large area myelin injury.

Statistics

Statistical analyses were performed with the Prism software version 9.0 (GraphPad). Data are presented as means ± SDs. One-way or two-way ANOVA was used to determine differences between groups and Tukey's post hoc test was used to determine differences between two pairs in multiple groups. The correlation between two variables was evaluated using Pearson's correlation test. $P < 0.05$ was considered statistically significant.

Results

Silence of the Efficient shRNA-Mediated B7-H4 Gene in C3H10 Cell Lines

A specific shRNA against B7-H4 was used to stably deplete B7-H4 expression. After transfection of negative control (NC) or specific shRNA, Western blot analysis and immunofluorescent staining were employed to evaluate interference efficiency. The data showed that B7-H4 protein levels decreased significantly in C3H10 cells (Fig. 1A). The same trend was observed for immunofluorescent staining (Fig. 1B). Furthermore, we detected the expression of B7-H4 bound to the membrane in each group by flow cytometry (Fig. 1C). Data confirmed that B7-H4 was downregulated by approximately 45% in shRNA-B7-H4 transfected cells compared to negative control transfected cells.

Knockdown of B7-H4 Induced Apoptosis of C3H10 Cells

To investigate the effect of B7-H4 on cell apoptosis in C3H10 cells, each group of cells was stained with Annexin-PE and 7-AAD and then detected by flow cytometry. As shown in Fig. 2A, B, the percentage of apoptotic cells was significantly higher in the C3H10-B7-H4sh group compared to the

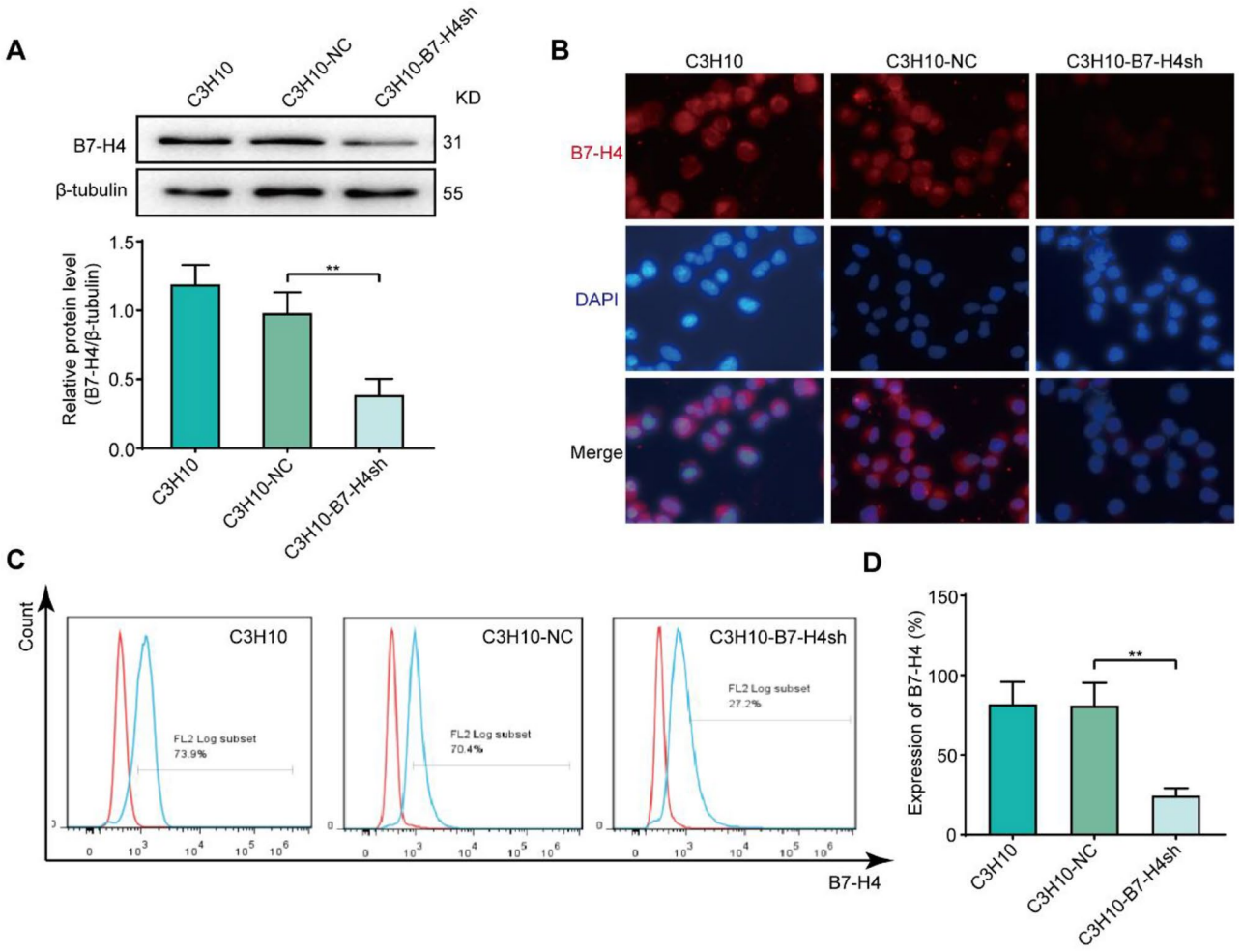

Fig. 1 Evaluation of the effect of shRNA silencing on B7-H4 in C3H10 cells. (**A**) Transfection efficiency of B7-H4 shRNA was analyzed by Western blotting. Quantification of Western blot as shown. (**B**) Representative images from immunofluorescence analysis of the efficiency of shRNA transfection on the expression of B7-H4. (**C**) Three groups of cells were harvested and analyzed by flow cytometry 48 h after transfection to further assess the efficiency of B7-H4 shRNA. (**D**) The statistical result of the flow cytometry analysis. (**A**) C3H10-B7-H4sh vs. C3H10-NC, $^{**}p < 0.01$; (**D**) C3H10-B7-H4sh vs. C3H10-NC, $^{**}p < 0.01$

C3H10-NC group. Subsequently, we detected apoptotic-related proteins to identify the underlying pro-apoptotic mechanisms in C3H10 cells. The results showed that the knockdown of B7-H4 resulted in upregulation of Bax, cleaved caspase3, and caspase9, and downregulation of Bcl-2 by Western blotting (Fig. 2C–H). These results suggest that B7-H4 depletion has an inhibitory effect on proliferation and could induce cell apoptosis in C3H10 cells.

The Proliferation Capacity of C3H10 Cells was Impaired and was Arrested in the G0/G1 Phase after the Knockdown of B7-H4

To investigate the role of B7-H4 in cell proliferation of C3H10 cells, we performed the cell count and CCK8 assays. Cell count and CCK8 assays showed that B7-H4 knockdown significantly suppressed the proliferation rate of C3H10 cells on day 3 (Fig. 3A, B). Stable cell cycle is important for cell proliferation. After finding the effect of downregulation of B7-H4 on C3H10 cell proliferation, we performed cell cycle analysis by flow cytometry. As shown in Fig. 3C, D, cells in the G0/G1 phase accumulated significantly after downregulation of B7-H4 compared to the C3H10-NC group. In the C3H10-B7-H4sh group, a greater proportion of C3H10 cells was reminded in the G0/G1 phase, while fewer cells were in the S phase.

Next, we detected the expression levels of cell cycle–related proteins by Western blotting (Fig. 3E). When B7-H4 was downregulated, cyclin D1 protein levels were acutely inhibited. These results indicate that B7-H4 knockdown disrupts the cell cycle of C3H10 cells, arresting them in the G0/G1 phase.

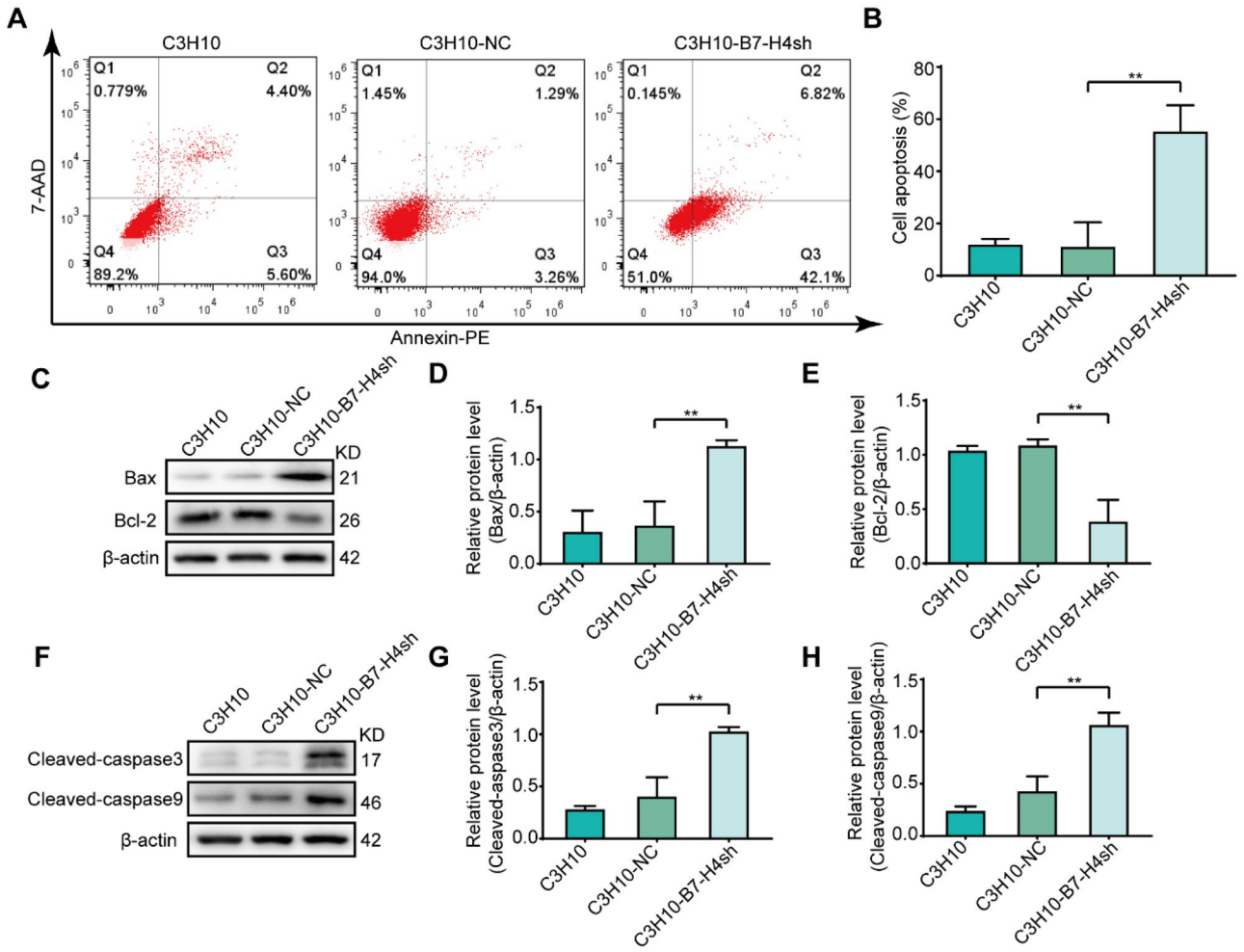

Fig. 2 Effect of B7-H4 downregulation on apoptosis in C3H10 cells. (**A**) Representative images of flow cytometry analysis of Annexin V-PE/7ADD staining. (**B**) The statistical result of the flow cytometry analysis. (**C**) The expression of Bax and Bcl-2 was analyzed in C3H10 cells by Western blotting. (**D**) Statistical results for Bax protein expression levels. (**E**) Statistical results for Bcl-2 protein expression levels. (**F**) The expression of cleaved-caspase3 and caspase9 was analyzed in C3H10 cells by Western blotting. (**G**) Statistical results for cleaved-caspase3 protein expression levels. (**H**) Statistical results for caspase9 protein expression levels. β-actin was used for standardization. (**D**) C3H10-B7-H4sh vs. C3H10-NC, $^{**}p<0.01$; (**E**) C3H10-B7-H4sh vs. C3H10-NC, $^{**}p<0.01$; (**G**) C3H10-B7-H4sh vs. C3H10-NC, $^{**}p<0.01$; (**H**) C3H10-B7-H4sh vs. C3H10-NC, $^{**}p<0.01$

B7-H4 Depletion Aggravated Symptoms and Spinal Cord Pathology in Mice Affected by EAE after Transplantation of C3H10 Cells

A previous study showed that bone marrow MSC transplantation (BM-MSC) can prevent the development of EAE. To further confirm that the downregulation of B7-H4 inhibited cell proliferation and its effect on the immunoregulation of C3H10 cells, we established a disease model by immunizing female C57BL/6 mice with MOG 35–55, and then the mice were injected intraperitoneally (i.p.) with EGFP-labeled C3H10 cells on day 7 (Fig. 4A). As indicated by immunofluorescent staining, $EGFP^+$ C3H10 cells were found in the area of spinal cord lesions (Fig. 4B). The mean clinical score was significantly higher in the C3H10-B7-H4sh group on day 10 compared to the C3H10 group. Daily monitoring of clinical scores showed that downregulation of B7-H4 could result in a distinct suppression of the immunoregulatory effect of C3H10 cells (Fig. 4D, E). To further investigate the role of B7-H4 in C3H10 cells, we detected inflammatory infiltration and demyelination changes in the spinal cord by LFB staining and H&E staining. Significant inflammatory infiltration and demyelination were shown in the C3H10-B7-H4sh group (Fig. 4F, H). Similarly, inflammatory infiltration and demyelination scores were significantly higher in mice transplanted with C3H10-B7-H4sh cells (Fig. 4G, I). Collectively, these results suggest that B7-H4 is essential for the immunoregulatory effect of C3H10 cells.

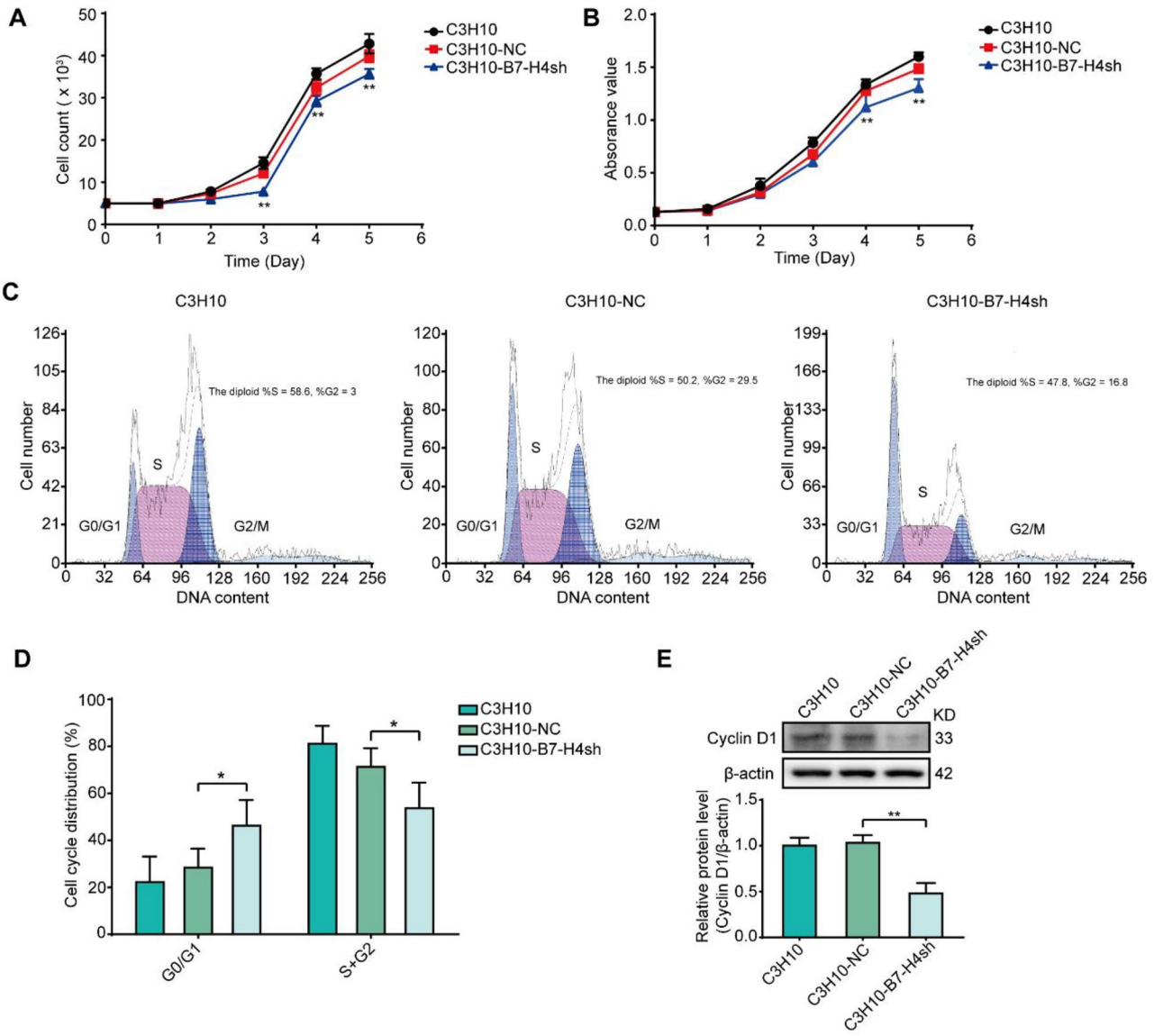

Fig. 3 Effect of B7-H4 downregulation on C3H10 cell proliferation. (**A**) Cell counts were measured at 0-, 1-, 2-, 3-, 4-, and 5-day time-points after B7-H4 shRNA transfection by using hemocytometer. (**B**) The viability of C3H10 cells was detected by the CCK-8 kit at 0-, 1-, 2-, 3-, 4-, and 5-day time-points after B7-H4 shRNA transfection. (**C**) The cell cycle distribution of C3H10 cells was identified by flow cytometry after transfection of B7-H4 shRNA. (**D**) The statistical result of the flow cytometry analysis. (**E**) The expression of Cyclin D1 was analyzed in C3H10 cells by Western blotting. β-actin was used for standardization. Quantification of Western blotting as shown. (**A**) Day 3: C3H10-B7-H4sh vs. C3H10-NC, $^{**}p<0.01$; day 4: C3H10-B7-H4sh vs. C3H10-NC, $^{**}p<0.01$; day 5: C3H10-B7-H4sh vs. C3H10-NC, $^{*}p<0.05$; (**B**) day 4: C3H10-B7-H4sh vs. C3H10-NC, $^{**}p<0.01$; day 5: C3H10-B7-H4sh vs. C3H10-NC, $^{*}p<0.05$; (**D**) C3H10-B7-H4sh vs. C3H10-NC, $^{*}p<0.05$; (**E**) C3H10-B7-H4sh vs. C3H10-NC, $^{**}p<0.01$

B7-H4 Depletion Attenuated the Immunoregulatory Effect of C3H10 Cells In Vivo

We then investigated the mechanisms by which depletion of B7-H4 exacerbates EAE. We first determined whether B7-H4 influenced the pathological process of EAE by activating microglia. In particular, downregulation of B7-H4 increased the amount of Iba1$^+$ microglia (Fig. 5A, B). Next, we determined the number of B7-H4$^+$ cells and PD-L1$^+$ cells in the spinal cord in each group. As shown in Fig. 5A, C, D, B7-H4 depletion decreased the number of B7-H4$^+$ cells and increased the number of PD-L1$^+$ cells. Furthermore, since C3H10 cells have mild immunogenicity, we detected the number of CD3$^+$ T cells and CD20$^+$ B cells. B7-H4 downregulation markedly increased the number of CD3$^+$ T cells in the C3H10-B7-H4sh group compared to the C3H10-NC group (Fig. 5A, E). Similarly, downregulation of B7-H4 markedly increased the number of CD20$^+$ B cells

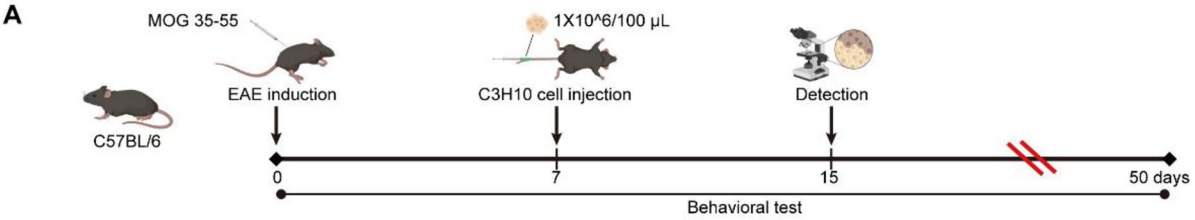

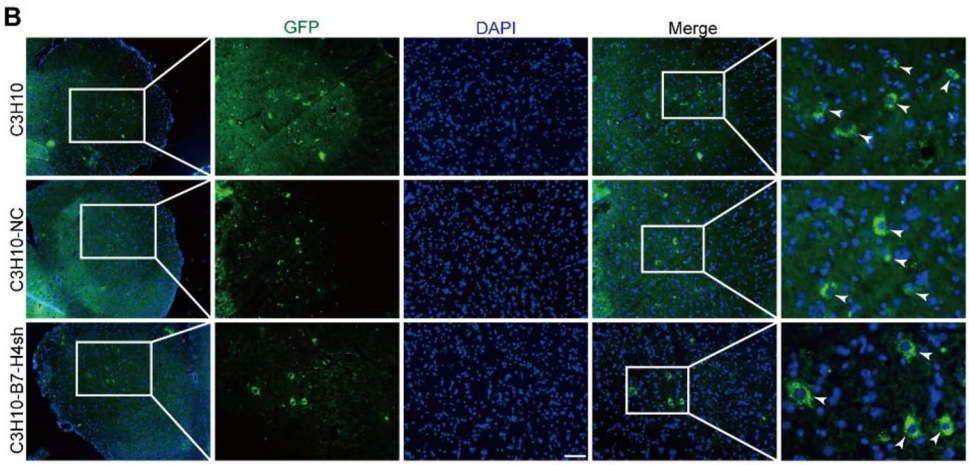

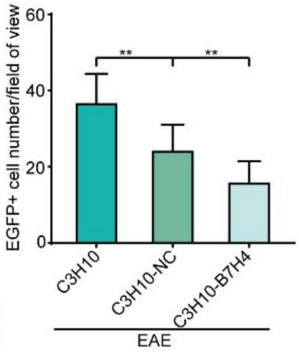

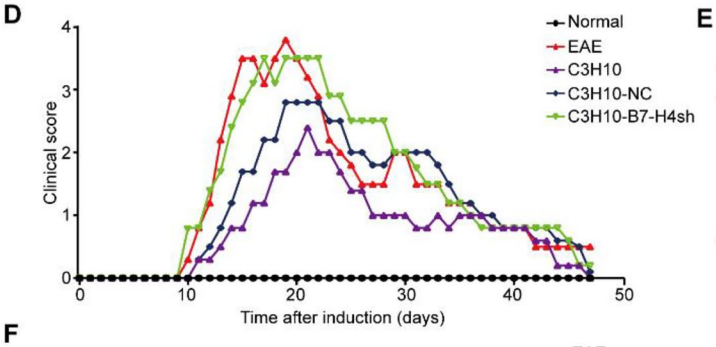

E

Groups	Onset of illness	Peak of illness	Mean clinical score
EAE	6.5±1.12	18.8±1.47	2.98±1.04
C3H10	12.4±1.35	23.7±1.34	1.03±0.57
C3H10-NC	11.6±0.89	23.5±1.35	1.15±0.49
C3H10-B7-H4sh	9.2±1.62	19.4±1.43	2.62±0.82

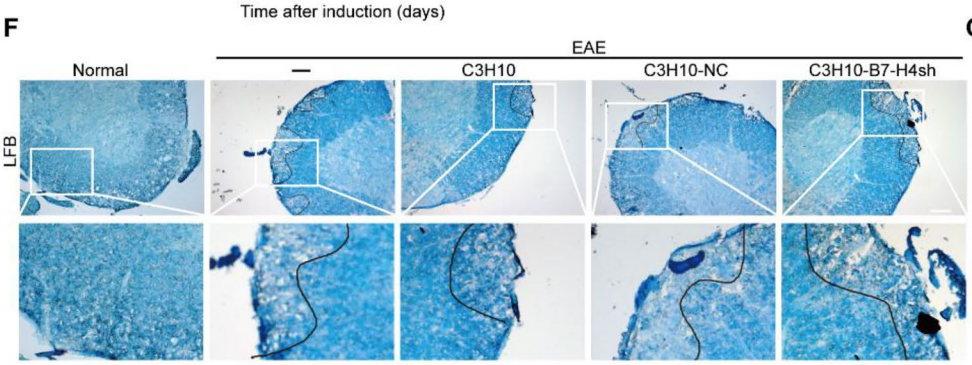

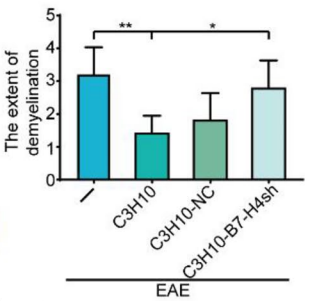

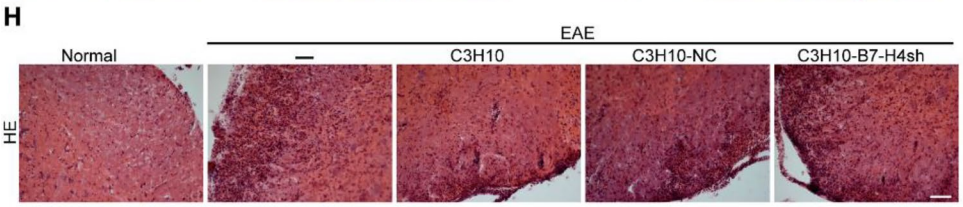

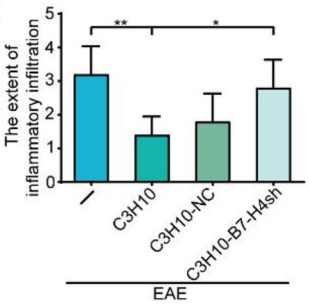

◂**Fig. 4** B7-H4 depletion aggravated symptoms and spinal cord pathology in mice affected by EAE after C3H10 cell transplantation. (**A**) C3H10 cell transplantation workflow. (**B**) The detection of C3H10 cells ($EGFP^+$, green) in the spinal cord. Arrows point to EGFP positive C3H10 cells (scale bar = 100 μm). (**C**) Cell counts of EGFP positive C3H10 cells in each field of view. (**D**) Mean clinical score. EAE mice were injected intravenously with 1×10^6 (100 μL) C3H10, C3H10-NC, or C3H10-B7-H4sh cells on day 7. (**E**) Evaluation of disease progression and neurological deficit scores. Values were expressed as mean ± SD. (**F**) Fifteen days after EAE, spinal cords were harvested from mice and stained with LFB staining (scale bar = 200 μm). (**G**) Histological scores for the degree of demyelination. (**H**) Fifteen days after EAE, spinal cords were harvested from mice and stained with HE staining (scale bar = 200 μm). (**H**) Histological scores for the extent of inflammation infiltration. (**C**) C3H10-NC vs. C3H10, $^{**}p < 0.01$; C3H10-B7-H4sh vs. C3H10-NC, $^{**}p < 0.01$. (**D**) EAE vs. normal, $^{**}p < 0.01$; C3H10 vs. EAE, $^{**}p < 0.01$; C3H10-B7-H4sh vs. C3H10-NC, $^{**}p < 0.01$. (**G**) C3H10 vs. EAE, $^{**}p < 0.01$; C3H10-B7-H4sh vs. C3H10, $^{*}p < 0.05$. (**I**) C3H10 vs. EAE, $^{**}p < 0.01$; C3H10-B7-H4sh vs. C3H10, $^{*}p < 0.05$

in the C3H10-B7-H4sh group compared to the C3H10-NC group (Fig. 5A, F). These suggest that B7-H4 mediates the regulation of the immune response of C3H10 cells in vivo.

Discussion

MSCs have unique immunomodulatory properties, and the previous study provides evidence that MSCs are a potential therapeutic target in various diseases (Yu et al. 2021; Levoux et al. 2020; Kuang et al. 2020). MSCs can self-renew and differentiate into a variety of different cell types for neurorestoration (Chan et al. 2018; Mao et al. 2006). However, preclinical research on MSC therapy remains controversial, especially the difficulty in clinical translation (Levy et al. 2020; Rolfes et al. 2020), forcing us to need more evidence to verify. In the current study, we confirm that transplantation of C3H10 T1/2 cells significantly improved the extent of inflammatory infiltration and demyelination in the spinal cord, delayed the onset, and reduced the neurological score of EAE mice. Therefore, transplantation of C3H10 T1/2 cells is effective in treating autoimmune diseases, providing compelling evidence for the therapy of MSCs.

Our previous research reported that B7-H4 can be stably expressed in human bone marrow–derived MSCs (Xue et al. 2010), but the characteristic of B7-H4 in MSC remain unclear. Consistently, we also found that C3H10 T1/2 cells can express B7-H4. Therefore, we employ C3H10 to investigate the effect of downregulation of B7-H4 on MSCs. Previous studies reveal that B7-H4 is negatively regulatory molecular in T lymphocytes (Wang and Wang 2020). And apoptosis induced by B7-H4 silencing is associated with the capacity for self-renewal, differentiation, and proliferation (Kang et al. 2017; Mo et al. 2013). B7-H4 might be a key regulator of these processes. Our data also showed that B7-H4-shRNA decreased the expression of antiapoptotic proteins and increased the expression of apoptotic proteins. Consistent with previous reports, we also found that B7-H4-shRNA induced cell cycle arrest in C3H10 T1/2 cells. However, more and more studies have demonstrated that the negative costimulatory molecule not only promoted apoptosis, but also affected autophagy (Hao et al. 2020). B7-H4 mediates multiple signaling pathways, such as the PI3K, PTEN, IL6, and VEGFA signaling pathways (Hao et al. 2020; Li et al. 2020; Xia et al. 2017; Yao et al. 2016), to regulate the occurrence of diseases. Therefore, the role of BH4 in various diseases needs further research to clarify.

In our study, we also detected the effect of B7-H4 depletion on the immunomodulatory effect of MSCs. As previously reported, MSCs have excellent immunoregulatory capabilities (Chan et al. 2018; Mao et al. 2006). MSC therapy can perform anti-inflammatory and tissue repair in vivo. MSCs can reduce microglial activation and reduce the degree of demyelination, while downregulation of B7-H4 exacerbated neurological dysfunction. Pathological examination of the spinal cord revealed that GFP + cells were present in areas surrounding spinal cord lesions. On the contrary, no cells with green fluorescence were observed in the non-diseased areas. In local lesion areas of the spinal cord, the number of GFP + cells was significantly reduced after downregulation of B7-H4 expression. The above phenomena indicate that cells transplanted by tail vein injection were able to migrate through the blood–brain barrier (BBB) to the area of the lesion and survive. And the number of C3H10 T1/2 cells in local lesion areas could be related to an increase in the severity of EAE. Autopsy data show that a large number of activated microglia are present in the brain lesion tissues of MS patients (Sbai et al. 2010). The activated microglia secrete inflammatory cytokines and other active substances, thus participating in the pathogenesis of MS, and inhibition of microglia activation significantly improves clinical symptoms (Sheremata et al. 2008; Marcos-Ramiro et al. 2014). In the present study, we found that downregulation of B7-H4 significantly limited the inhibitory effects of C3H10 T1/2 cells on microglial activation and migration. We also observed a decrease in the number of cells positive for PD-L1 and B7-H4 in the C3H10-B7-H4sh group. We speculated that the B7-H4 protein expressed in C3H10 cells affected the expression of the negative costimulatory molecules B7-H4 and PD-L1 in the spinal cord microenvironment. Therefore, B7-H4 is a key molecular marker for MSCs and can be used as an immune checkpoint in MS. Furthermore, as previously described, in multiple sclerosis, brain damage is primarily a clonal expansion of $CD3^+$ T cells and $CD20^+$ B cell infiltration (Hohlfeld et al. 2016; Machado-Santos et al. 2018; Gottlieb et al. 2022). Similarly, significant infiltration of $CD3^+$ T cells and $CD20^+$ B cells was also reported in the MOG35-55-induced EAE

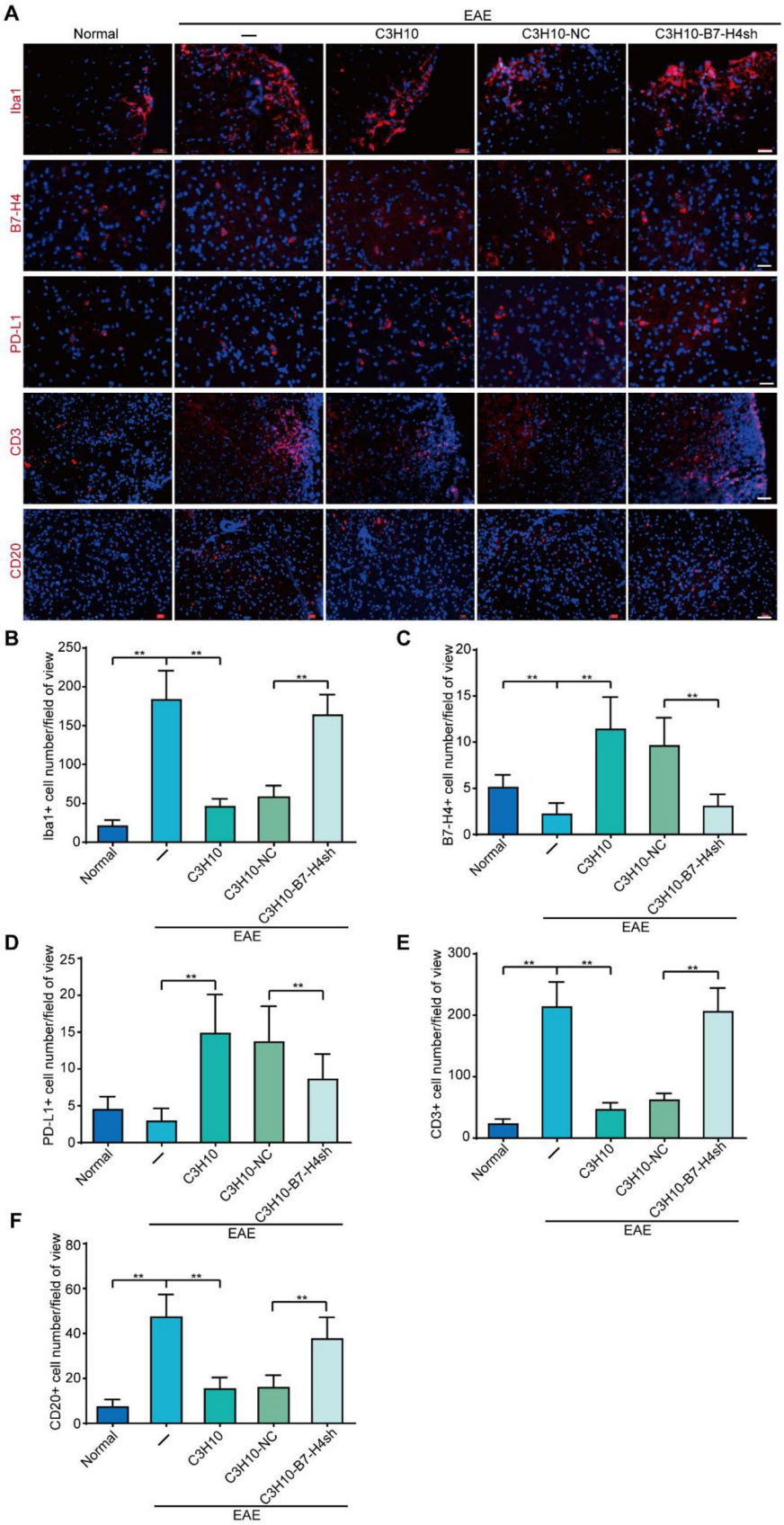

Fig. 5 B7-H4 depletion attenuated the immunoregulatory effect of C3H10 cells in vivo. (**A**) Representative fluorescent images of cells Iba1$^+$ (red), B7-H4$^+$ (red), PD-L1$^+$ (red), CD3$^+$ (red), and CD20$^+$ (red) in the spinal cord after treatment with C3H10, C3H10-NC, and C3H10-B7-H4sh (scale bar = 100 μm). (**B**) Statistical results of Iba1$^+$ immunofluorescence staining. (**C**) Statistical results of B7-H4$^+$ immunofluorescence staining. (**D**) Statistical results of PD-L1$^+$ immunofluorescence staining. (**E**) Statistical results of CD3$^+$ immunofluorescence staining. (**F**) Statistical results of CD20$^+$ immunofluorescence staining. (**B**) EAE vs. normal, $^{**}p < 0.01$; C3H10 vs. EAE, $^{**}p < 0.01$; C3H10-B7-H4sh vs. C3H10-NC, $^{**}p < 0.01$. (**C**) EAE vs. normal, $^{**}p < 0.01$; C3H10 vs. EAE, $^{**}p < 0.01$; C3H10-B7-H4sh vs. C3H10-NC, $^{**}p < 0.01$. (**D**) C3H10 vs. EAE, $^{**}p < 0.01$; C3H10-B7-H4sh vs. C3H10-NC, $^{**}p < 0.01$. (**E**) EAE vs. normal, $^{**}p < 0.01$; C3H10 vs. EAE, $^{**}p < 0.01$; C3H10-B7-H4sh vs. C3H10-NC, $^{**}p < 0.01$. (**F**) EAE vs. normal, $^{**}p < 0.01$; C3H10 vs. EAE, $^{**}p < 0.01$; C3H10-B7-H4sh vs. C3H10-NC, $^{**}p < 0.01$

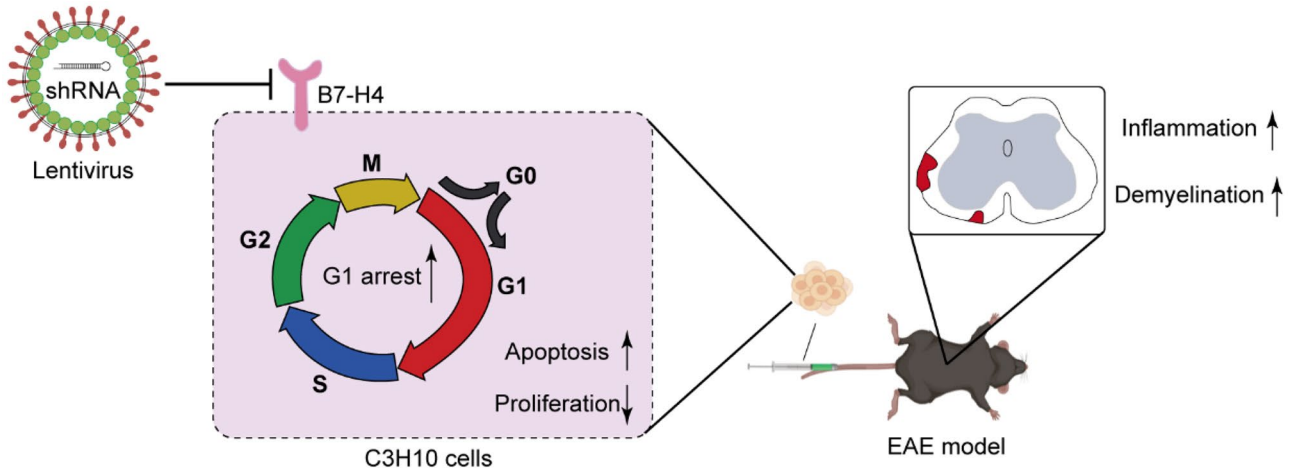

Fig. 6 Schematic representation of the effect of B7-H4 depletion in C3H10 cells

model (Virgili et al. 2011; Makar et al. 2015), and our results showed the same inflammatory burden, and transplantation of C3H10 cells significantly reduced this inflammatory burden. Interestingly, when we downregulated B7-H4 but increased the number of $CD3^+$ T cells and $CD20^+$ B cells infiltrating cells, this proved that after downregulating B7-H4, the immunomodulatory ability of C3H10 was destroyed, and B7-H4 is an important molecule for C3H10 to exert immunomodulatory ability.

This study has some limitations. First, healthy female mice were used to build EAE models in our study, which do not maximally simulate the age distribution of MS. The literature revealed that 14% of MS patients were 65 years old (Minden et al. 2004). Furthermore, the relationship between B7-H4 and MS requires continued studies for its future elucidation, because our research found that after MSC therapy, mice with a better prognosis expressed higher negative costimulatory molecules, such as B7-H4 or PD-L1. Regrettably, we just demonstrated the effect of B7-H4 depletion on C3H10 T1/2 cells and did not compare the efficacy of B7-H4 overexpression and B7-H4 depletion.

Conclusions

Our study provides compelling evidence for the availability of MSC therapy. In addition, our study provided evidence that B7-H4 could be an immune checkpoint in autoimmune diseases. B7-H4 was constitutively highly expressed in C3H10 T1/2 cells, and B7-H4 depletion induced apoptosis and impaired cell proliferation by arresting in phase G0/G1 in C3H10 T1/2 cells. Consistently, depletion of B7-H4 attenuated the immunomodulatory effect of C3H10 T1/2 cells and increased changes in inflammatory infiltration and demyelination in the EAE model (Fig. 6). Thus, B7-H4 may act as an important quality control molecule for C3H10 T1/2 cells and serve as a target molecule that can be artificially regulated. The present study reveals for the first time the important role of B7-H4 in MSCs and provides new clues for the application of MSCs in the treatment of autoimmune diseases.

Supplementary Information The online version contains supplementary material available at https://doi.org/10.1007/s12640-022-00509-3.

Funding This work is supported by grants from the National Natural Science Foundation of China (81273269, 81601011), the Jiangsu Province Key Research and Development Program (Social Development) (BE2019666), and the Natural Science Foundation of Jiangsu Province (BK20211075).

Data Availability The data used to support the findings of this study are available from the corresponding author upon request.

Declarations

Competing Interests The authors declare no competing interests.

References

Chan CKF, Gulati GS, Sinha R et al (2018) Identification of the human skeletal stem cell. Cell 175(1):43-56.e21

Collins M, Ling V, Carreno BM (2005) The B7 family of immune-regulatory ligands. Genome Biol 6(6):223

Faissner S, Plemel JR, Gold R, Yong VW (2019) Progressive multiple sclerosis: from pathophysiology to therapeutic strategies. Nat Rev Drug Discovery 18(12):905–922

Gottlieb A, Pham HPT, Lindsey JW (2022) Brain antigens stimulate proliferation of T lymphocytes with a pathogenic phenotype in multiple sclerosis patients. Front Immunol 13:835763

Greaves P, Gribben JG (2013) The role of B7 family molecules in hematologic malignancy. Blood 121(5):734–744

Gugliandolo A, Bramanti P, Mazzon E (2020) Mesenchymal stem cells in multiple sclerosis: recent evidence from pre-clinical to clinical studies. Int J Mol Sci 21(22)

Hao TT, Liao R, Lei DL, Hu GL, Luo F (2020) Inhibition of B7–H4 promotes hepatocellular carcinoma cell apoptosis and autophagy through the PI3K signaling pathway. Int Immunopharmacol 88:106889

Hohlfeld R, Dornmair K, Meinl E, Wekerle H (2016) The search for the target antigens of multiple sclerosis, part 2: CD8+ T cells, B cells, and antibodies in the focus of reverse-translational research. Lancet Neurol 15(3):317–331

Jeon H, Vigdorovich V, Garrett-Thomson SC et al (2014) Structure and cancer immunotherapy of the B7 family member B7x. Cell Rep 9(3):1089–1098

Jia Y, Zhang D, Li H et al (2021) Activation of FXR by ganoderic acid A promotes remyelination in multiple sclerosis via anti-inflammation and regeneration mechanism. Biochem Pharmacol 185:114422

Kang FB, Wang L, Sun DX et al (2017) B7–H4 overexpression is essential for early hepatocellular carcinoma progression and recurrence. Oncotarget 8(46):80878–80888

Kuang Y, Zheng X, Zhang L et al (2020) Adipose-derived mesenchymal stem cells reduce autophagy in stroke mice by extracellular vesicle transfer of miR-25. J Extracell Vesicles 10(1):e12024

Levoux J, Prola A, Lafuste P et al (2020) Platelets facilitate the wound-healing capability of mesenchymal stem cells by mitochondrial transfer and metabolic reprogramming. Cell Metab 33(2):283–299

Levy O, Kuai R, Siren EMJ et al (2020) Shattering barriers toward clinically meaningful MSC therapies. Sci Adv 6(30):eaba6884

Li C, Zhan Y, Ma X, Fang H, Gai X (2020) B7–H4 facilitates proliferation and metastasis of colorectal carcinoma cell through PI3K/Akt/mTOR signaling pathway. Clin Exp Med 20(1):79–86

Machado-Santos J, Saji E, Tröscher AR et al (2018) The compartmentalized inflammatory response in the multiple sclerosis brain is composed of tissue-resident CD8+ T lymphocytes and B cells. Brain 141(7):2066–2082

Makar TK, Gerzanich V, Nimmagadda VK et al (2015) Silencing of Abcc8 or inhibition of newly upregulated Sur1-Trpm4 reduce inflammation and disease progression in experimental autoimmune encephalomyelitis. J Neuroinflammation 12:210

Mao JJ, Giannobile WV, Helms JA et al (2006) Craniofacial tissue engineering by stem cells. J Dent Res 85(11):966–979

Marcos-Ramiro B, Oliva Nacarino P, Serrano-Pertierra E et al (2014) Microparticles in multiple sclerosis and clinically isolated syndrome: effect on endothelial barrier function. BMC Neurosci 15:110

Minden SL, Frankel D, Hadden LS, Srinath KP, Perloff JN (2004) Disability in elderly people with multiple sclerosis: an analysis of baseline data from the Sonya Slifka Longitudinal Multiple Sclerosis Study. NeuroRehabilitation 19(1):55–67

Mo LJ, Ye HX, Mao Y, Yao Y, Zhang JM (2013) B7–H4 expression is elevated in human U251 glioma stem-like cells and is inducible in monocytes cultured with U251 stem-like cell conditioned medium. Chin J Cancer 32(12):653–660

Pfeuffer S, Ruck T, Kleinschnitz C, Wiendl H, Meuth SG (2016) Failed, interrupted and inconclusive trials on relapsing multiple sclerosis treatment: update 2010–2015. Expert Rev Neurother 16(6):689–700

Podojil JR, Liu LN, Marshall SA et al (2013) B7–H4Ig inhibits mouse and human T-cell function and treats EAE via IL-10/Treg-dependent mechanisms. J Autoimmun 44:71–81

Prasad DV, Richards S, Mai XM, Dong C (2003) B7S1, a novel B7 family member that negatively regulates T cell activation. Immunity 18(6):863–873

Rolfes L, Pawlitzki M, Pfeuffer S et al (2020) Failed, interrupted, or inconclusive trials on immunomodulatory treatment strategies in multiple sclerosis: update 2015–2020. BioDrugs 34(5):587–610

Sbai O, Ould-Yahoui A, Ferhat L et al (2010) Differential vesicular distribution and trafficking of MMP-2, MMP-9, and their inhibitors in astrocytes. Glia 58(3):344–366

Sheremata WA, Jy W, Horstman LL, Ahn YS, Alexander JS, Minagar A (2008) Evidence of platelet activation in multiple sclerosis. J Neuroinflammation 5:27

Song X, Zhou Z, Li H et al (2020) Pharmacologic suppression of B7–H4 glycosylation restores antitumor immunity in immune-cold breast cancers. Cancer Discov 10(12):1872–1893

Vaughn CB, Jakimovski D, Kavak KS et al (2019) Epidemiology and treatment of multiple sclerosis in elderly populations. Nat Rev Neurol 15(6):329–342

Virgili N, Espinosa-Parrilla JF, Mancera P et al (2011) Oral administration of the KATP channel opener diazoxide ameliorates disease progression in a murine model of multiple sclerosis. J Neuroinflammation 8:149

Wang JY, Wang WP (2020) B7–H4, a promising target for immunotherapy. Cell Immunol 347:104008

Xia F, Zhang Y, Xie L et al (2017) B7–H4 enhances the differentiation of murine leukemia-initiating cells via the PTEN/AKT/RCOR2/RUNX1 pathways. Leukemia 31(10):2260–2264

Xue Q, Luan XY, Gu YZ et al (2010) The negative co-signaling molecule b7–h4 is expressed by human bone marrow-derived mesenchymal stem cells and mediates its T-cell modulatory activity. Stem Cells Dev 19(1):27–38

Yao Y, Ye H, Qi Z et al (2016) B7–H4(B7x)-Mediated cross-talk between glioma-initiating cells and macrophages via the IL6/JAK/STAT3 pathway lead to poor prognosis in glioma patients. Clin Cancer Res 22(11):2778–2790

Yu M, Ma L, Yuan Y et al (2021) Cranial suture regeneration mitigates skull and neurocognitive defects in craniosynostosis. Cell 184(1):243–256.e218